JOURNAL OF APPLIED PHYSICS **121**, 235302 (2017)

Metal-insulator transition and nonlinear optical response of sputter-deposited V_3O_5 thin films

Armando Rúa, Ramón D. Díaz, Nardeep Kumar, Sergiy Lysenko, and Félix E. Fernández[a)]
Department of Physics, University of Puerto Rico, Mayagüez, Puerto Rico 00681-9000, USA

(Received 27 February 2017; accepted 4 June 2017; published online 19 June 2017)

The compound V_3O_5, a member of the vanadium oxide Magnéli series, exhibits a metal-insulator transition near 430 K, the highest known temperature value among all vanadium oxides. It has been studied before mainly in single-crystal form, and for the very few cases in which thin films have been fabricated before, the procedure has required extensive post-deposition annealing of other oxides or vanadium metal at high temperatures in tightly controlled atmospheres. For the present work, V_3O_5 films were deposited directly on SiO_2 glass substrates, without subsequent annealing, by DC magnetron sputtering. X-ray diffraction study of the samples evidenced oxygen deficiency, accommodated by oxygen vacancies. Resistivity measurements from 300 to 500 K revealed the metal-insulator transition by $T_c \sim 430$ K, with an associated resistivity change by a factor of 20, and no detectable hysteresis in heating-cooling cycles, in agreement with most single-crystal studies. Resistivity values obtained were, however, lower than published results for bulk crystal values, particularly at temperatures below T_c. This was attributed to conduction electrons generated by the oxygen vacancies. Gradual resistivity increase in a very thin sample, through heating in air at temperatures up to 500 K, lends support to this argument. Using a pump-probe scattering technique, the V_3O_5 films were also probed for ultrafast nonlinear optical response. A reduction in the transient relative scattered light signal was recorded, which reached –10% within ~800 fs. This observed response, likely related to the photoinduced insulator-to-metal phase transition, should stimulate additional interest in this material. *Published by AIP Publishing.*
[http://dx.doi.org/10.1063/1.4986486]

INTRODUCTION

Because vanadium is a polyvalent transition metal, it can form a large number of oxide compounds. Among these, the vanadium Magnéli phases are a series of stoichiometric compounds with compositions V_nO_{2n-1}, where $n = 3, 4, \ldots 9$. It is bordered by vanadium sesquioxide (V_2O_3) and vanadium dioxide (VO_2), in which the vanadium valence is, respectively, three and four. Through the series, the number of V^{3+} cations per formula unit is always two, while the number of V^{4+} cations increases from one (in V_3O_5) to seven (in V_9O_{17}).[1] In terms of crystal structure, the series shares characteristics with corundum (as does high-V_2O_3) and rutile (as does high-VO_2). The compounds are stable at least up to 1600 K.[2] Except for V_7O_{13}, which remains metallic, all members of the series exhibit reversible metal-insulator transitions as the temperature is lowered, followed by antiferromagnetic ordering at a lower temperature. The transition temperature (T_c) generally decreases (except for V_6O_{11}) as the number of V^{4+} cations in the structure increases. The first member in the series, V_3O_5, has the highest T_c, near 430 K.[1] Unlike the others in the series, but like VO_2, it exhibits non-metallic conduction at ambient and lower temperatures. These two materials are the only two vanadium oxides known to have T_c values higher than room temperature. While the conductivity change in V_3O_5 is not as pronounced as in VO_2, its relatively high T_c (~130° above room temperature) makes it interesting for possible device applications, including oxide electronics.[3,4] In complementary metal-oxide-semiconductor (CMOS) devices, for example, as sizes have been scaled down, junction temperatures tend to be higher and cooling requirements can become more demanding.[5] Incorporation of VO_2 in order to employ its resistive switching characteristics will likely require active cooling of devices to avoid unintended thermally induced switching. Instead, devices incorporating V_3O_5 may operate at much higher junction temperatures without encountering this issue.

The compound V_3O_5 was first reported by Andersson in 1954. Its crystal structure was initially determined a few years later,[6] and later corrected,[7,8] by Åsbrink *et al*. The structure of V_3O_5 at temperatures under T_c (low-V_3O_5) is monoclinic (space group P2/*c*) with four formula units per unit cell, and lattice parameters (room temperature values) $a = 9.859(1)$ Å, $b = 5.0416(5)$ Å, $c = 6.991(1)$ Å, and $\beta = 109.478(6)°$.[8] At temperatures over T_c (high-V_3O_5) the structure changes only slightly and remains monoclinic, with percentage changes in the lattice constants of approximately −0.13, −0.29, and +0.26 for *a*, *b*, and *c*, respectively, and a 0.053% increase in the β angle. However, the space group for the structure changes to the more symmetric I2/*c*, which is attested by the loss of all odd $h + k + l$ reflections in X-ray diffraction (XRD) patterns.

A change in conductivity near ~430 K was noticed as early as 1960 for a compound with $VO_{1.67}$ composition, and attributed to a phase transition.[9] More than a decade later,

a)Author to whom correspondence should be addressed: felix.fernandez@upr.edu

Terukov *et al*. studied the electrical characteristics of V_3O_5 single crystals grown by thermal transport and associated the insulator-to-metal transition with reordering of the cations.[10–12] The resistivity of these single crystals was found to be ~100 Ω cm at room temperature (ρ_{RT}), with decreasing values as the temperature increased, and a sudden drop by a factor of "up to 20" when the transition was reached. With further heating, conduction showed Arrhenius-type behavior, with a conductivity activation energy of 0.13 eV. On the basis of measurements of thermoelectric power and optical properties, these authors typified conduction at temperatures above T_c as metallic for the V_3O_5 crystals, even though it had to be considered a "poor metal". The relatively high resistivity for low-V_3O_5 has been attributed to localization of *d*-electrons, with delocalization being responsible for the drop in resistivity for high-V_3O_5.[12] The fact that resistivity continues to drop with increasing temperature after the transition to the "metallic" phase may be caused by temperature-dependent changes in the band overlap.[13]

Shortly after the initial publications by Terukov *et al*., Khoi *et al*.[14] reported similar results for a phase transition (at 420 K) in V_3O_5 single crystal samples, although their reported resistivities were one order of magnitude lower (ρ_{RT} ~10 Ω cm, for example). A similar resistivity change by a factor of ~20 (at 427 K), and ρ_{RT} ~30 Ω cm values, were also reported a few years later.[15] In this last case, a conductivity activation energy of 0.34 eV was determined for temperatures below 400 K. A much more recent report showed a resistivity change by a factor of only 8, with a very sharp transition (near 428 K), and ρ_{RT} ~300 Ω cm.[16] In this last case, a thermal hysteresis of 1.4 K was observed for the transition, and none outside this narrow transition zone. Most previous reports had either not commented on any observations of hysteresis, mentioned explicitly that none was observed,[11] or quoted a value of less than 0.5 K,[12] or "less than 0.5 K, if any."[14]

Very recent work has been reported on electric-field-induced resistive switching in V_3O_5 studied through current-voltage measurements in sintered polycrystalline bars (which included up to a few percent of either V_2O_3 or V_4O_7 phases) and in millimeter-sized single crystals. Room-temperature resistivities for the sintered samples in this study ranged from 80 to 1200 Ω cm.[17]

There are very few reports in the literature for V_3O_5 thin films. Because the stoichiometric range of V_3O_5 is just between $VO_{1.666}$ and $VO_{1.668 \pm 0.002}$,[11] attempts to fabricate films have been limited so far to cases in which films of either other vanadium oxides or vanadium metal have been annealed, at least in cases in which information about conditions were stated, for one to several days under a controlled atmosphere at high temperatures. In all cases, pure-phase or nearly pure-phase V_3O_5 has been claimed, as determined by XRD, although characterization details were not included. In the same publication in which they reported their observation of the metal-insulator transition in V_3O_5 crystals, Khoi *et al*.[14] showed results for resistivity measurements of V_3O_5 thin films produced by annealing VO_2 or V_2O_3 films deposited by RF sputtering. Unfortunately, the authors did not provide any other information about growth or annealing conditions and the report was apparently not followed by subsequent publications. The first detailed report for V_3O_5 thin films was published by Beresneva *et al*.[18] Their procedure required reducing ~200 nm thick V_2O_5 films by annealing them at nearly 1000 K for several days in sealed ampoules which included powdered two-phase (V_2O_5 and V_2O_3) vanadium oxides with prescribed proportions, and water vapor. The phase transition of the resulting films extended over at least ~40°, and resistivity change was nearly an order of magnitude, with the steepest descent by ~408 K. The room temperature resistivity was ~300 Ω cm. Much later, a similar technique was used to prepare V_3O_5 films by thermal oxidation, over 24 h, of thin vanadium metal foils sealed in ampoules.[19] The phase transition region of the resulting films showed a large change in conductivity of about two orders of magnitude, but extended over a very broad range of almost 100°. The temperature for the steepest descent was ~380 K, and the resistivity at room temperature was ~5 Ω cm. Thus, in summary, all previous results for V_3O_5 thin films demonstrate changes in resistivity through the transition of no less than about one order of magnitude, in agreement with most single crystal results. Unsurprisingly for thin film samples, the resistivity change through the transition was always much less abrupt than for single crystals, being spread out in temperature by at least several tens of degrees. From the given growth conditions, all V_3O_5 films reported so far have been surely polycrystalline, although this point was not often addressed, and crystallite sizes were not stated. Temperatures for the steepest descents through the transition were usually shifted down by tens of degrees from the T_c value for single crystals. This substantial shift was not explained, but could be related to several factors, including small crystallite sizes and deviations from the exact stoichiometry. For the present work, V_3O_5 thin films were deposited using a very direct approach, as we sought means to produce this promising material in a manner readily compatible with the current microelectronic fabrication technology.

SAMPLE PREPARATION

Thin film samples were deposited on glass (SiO_2) substrates by reactive DC magnetron sputtering from a vanadium (99.95% purity) target, without subsequent annealing. During reactive sputtering with oxygen, there are competing processes in which the metallic target becomes oxidized and the metal oxide is sputtered. As is well known, this competition causes a hysteresis loop which can make it difficult to obtain films with a desired composition.[20] For vanadium oxides, the task is not made any easier by the large variety of compounds which can result. Moreover, the very narrow stoichiometric range of V_3O_5 makes it one of the least promising candidates for direct growth by reactive sputtering. However, by characterization of the sputtering hysteresis loop and appropriate selection and control of growth conditions, it was expected that it would be possible to deposit nearly pure-phase as-grown V_3O_5 films. Growth conditions were adjusted so that the sputtering target remained in its "metallic" condition and just outside the hysteretic loop region. The distance between the 2″ diameter target and the substrates was 10 cm and the substrates were kept at

$T_s = 475\,^{\circ}C$ during growth. The background pressure was in the 10^{-5} Torr range, and the sputtering pressure was 20 mTorr, with argon and oxygen flows of 35.0 and 2.6 standard cubic centimeters per minute, respectively. The sputtering power was 300 W. After deposition was completed, gas flows and power to the sample heater were cut off, and the sample was left to cool in vacuum. No post-deposition treatment was applied to the samples. Sample thicknesses were measured with a stylus profilometer using steps created by masking the samples. The deposition rate obtained was ~16 nm/min. The thickness of samples for the characterization results reported here, except as noted, was 240 nm.

STRUCTURAL CHARACTERIZATION

X-ray diffraction θ–2θ scans of samples were recorded in a Bruker Discover D8 diffractometer using Cu K_α radiation. The result shown in Fig. 1 was recorded for over 18 h in order to detect and identify very low-intensity reflections. The very broad peak by $2\theta \sim 21^{\circ}$ is caused by the glass substrate. Excepting the two peaks indicated with asterisks in the scan, all can be closely assigned to low-V_3O_5 according to the Powder Diffraction File (PDF) 72–0977,[21] and relative intensities are in fair agreement with those given in the PDF, which evidences that the orientation of crystallites is approximately random. For clarity, the assigned indices shown in the figure are only those for isolated peaks which were used for further structural analysis. (The same result, but with all peaks indexed is presented as Fig. S1 in the supplementary material.) A few peaks are slightly shifted up or down in relation to the reference values. These shifts are attributed to anisotropic lattice deformation. Some peaks appear to be relatively broad (f.i., by $2\theta \approx 41^{\circ}$ and $\sim 69^{\circ}$) but in all these cases several V_3O_5 reflections are expected and are likely unresolved in the scan. From the integrated widths of main isolated V_3O_5 peaks in the θ–2θ scan, after subtracting the instrumental line broadening, Scherrer crystallite sizes were calculated. The results range from ~65 to ~180 nm, thus the vertical coherence length for microcrystallites is between ~1/4 and ~3/4 of the film thickness. The two extraneous peaks indicated in Fig. 1 are identified as the strongest V_2O_3 reflections: (104) and (116), according to indexing in PDF 85–1411.[22] No other phases were detected.

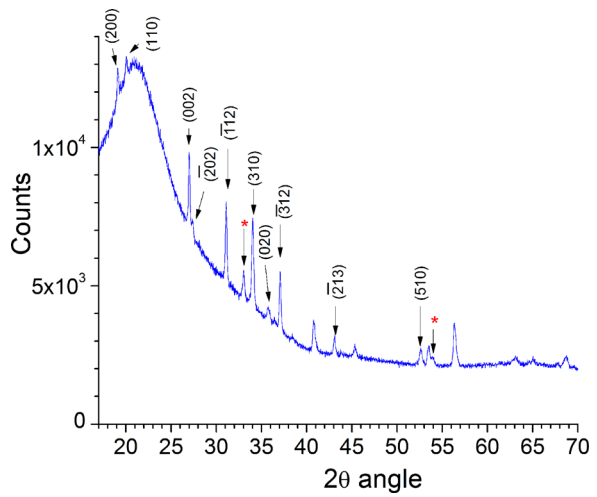

FIG. 1. Long-count XRD scan for a 240 nm thick sample. All reflections can be assigned to V_3O_5 except for the two indicated by asterisks, which correspond to the strongest reflections in V_2O_3. Indices are shown for selected V_3O_5 reflections (see text).

In the phase diagram for vanadium oxides, V_3O_5 is bordered by V_2O_3 and V_4O_7.[23] Hence, finding the first of these as impurity strongly suggests that the V_3O_5 in the film is oxygen-deficient. The fact that the two observed V_2O_3 peaks correspond to different reflection families indicates that the V_2O_3 crystallites are also randomly oriented, as could be expected. It is noted that in thinner films grown under the same conditions the observed intensity of these peaks was lower, in some cases with only the strongest (104) reflection showing, and in films thinner than ~100 nm no V_2O_3 peaks were detected. We do not interpret this to mean that in those last cases the V_3O_5 films are pure-phase, but that the concentration of V_2O_3 inclusions is likely too small to be detectable by XRD. This absence is then an indication that the concentration of V_2O_3 inclusions in the thicker films, grown under the same conditions, which did show its presence in XRD scans, is likely small.

Table I presents the *d*-spacings corresponding to clear and isolated V_3O_5 XRD peaks from the film (only those indexed in Fig. 1). The lattice parameters of the V_3O_5 unit cell, assuming its monoclinic structure, were calculated from this information. The results obtained for the *a*, *b*, *c*, and β angle are 9.830 Å, 5.024 Å, 7.018 Å, and 109.7°, respectively. This reveals that the unit cell is slightly distorted with respect to bulk V_3O_5 values, with angle β increasing by approximately 0.2°, while the lattice lengths are contracted along the *a* and *b* directions and extended along the *c* direction. From the values obtained, the volume of the unit cell is calculated to be 326.3 $Å^3$, which is about 0.4% lower than the bulk value. This slight contraction of the cell indicates that the expected oxygen deficiency is mainly accommodated by oxygen vacancies, and not by interstitial vanadium atoms. Thus, the thin film material composition may be better described as $V_3O_{5-\delta}$, with minor V_2O_3 inclusions. We note in passing that very recent results for first-principle calculations of formation energies of defects in VO_2 (M) show that oxygen vacancies, instead of vanadium interstitials, are energetically favored when this material is oxygen-

TABLE I. Indexing and *d*-spacings corresponding to main V_3O_5 peaks in Fig. 1.

d spacing (Å)		
Measured	PDF 72-0977	Index
4.628	4.6473	(200)
4.422	4.4316	(110)
3.304	3.2954	(002)
3.253	3.2472	($\bar{2}$02)
2.877	2.8721	($\bar{1}$12)
2.634	2.6396	(310)
2.512	2.5208	(020)
2.425	2.4233	($\bar{3}$12)
2.100	2.0965	($\bar{2}$13)
1.739	1.7441	(510)

deficient.[24] We suggest that the case will turn out to be the same in V_3O_5.

SURFACE TOPOGRAPHY

An Atomic Force Microscope (Park Scientific Autoprobe CP) was used to study the sample surface topography. A typical image is presented in Fig. 2 for a 3 μm × 3 μm scan in contact mode. The surface root-mean-square (*rms*) roughness over the full scan is 13 nm. The grain structure is fairly uniform, with lateral sizes of ∼300 nm, generally narrow spaces in between grains, and very few, if any, observable pores. This grain size is somewhat larger than film thickness and a few times larger than the estimated vertical coherence length for microcrystallites.

The preceding AFM results and the lack of preferential orientation revealed by XRD suggest film growth by coalescence of islands and subsequent development of a columnar structure with increasing diameter as the film thickens, which would be consistent with enough thermal energy for surface mobility of adatoms but not for bulk mobility. Because of the relatively high total gas pressure used during film growth, atoms arriving at the substrate, located 10 cm away from the target, are largely thermalized.[25] Hence adatom mobility should be mainly dependent on the substrate temperature. The fact that surface mobility is actually enabled and contributes to relatively large grain sizes may be justified by considering an empirical Structure Zone Model (SZM) similar to the one first proposed by Movchan and Demchishin for films deposited by electron beam evaporation.[26] In these models, the film morphology is characterized in terms of a few characteristic zones, and the main factor determining the resulting morphology is the ratio T_s/T_{melt}, where T_s is the substrate temperature during growth and T_{melt} is the melting temperature of the material being deposited, and both T_s and T_{melt} are stated in Kelvin. The Movchan–Demchishin model was later extended by Thornton for sputter-deposited pure metallic films by including the effects of the working gas pressure.[27] For compound films there are additional relevant factors, particularly when reactive sputtering is employed. A revised SZM for the case of sputter-deposited ZnO films was developed by Mirica *et al.*,[28] who demonstrated that, compared to the cases treated by Thornton, the limits between the different morphology zones are shifted to significantly lower substrate temperatures: that is, to lower values of the T_s/T_{melt} parameter. Bulk V_3O_5 is stable at temperatures up to ∼1900 K,[23,29] after which it likely decomposes. Using this value as an upper limit T_{max} for compound stability, instead of a melting temperature, the value of the ratio T_s/T_{max} was ∼0.4 during growth of the films prepared for the present work, and this may be taken as an indication that surface diffusion of adatoms during film growth was indeed likely, but not bulk diffusion.

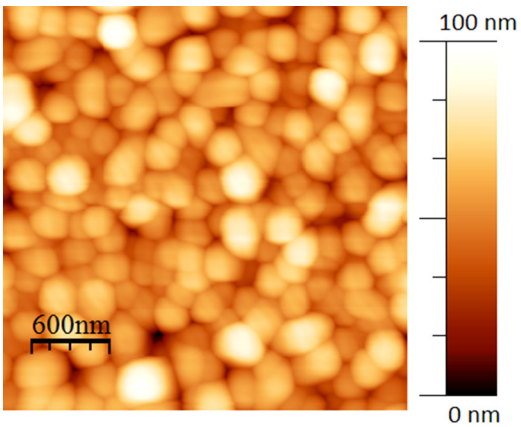

FIG. 2. AFM image (3 μm × 3 μm) of V_3O_5 film surface.

ELECTRICAL PROPERTIES

Sample resistivity (ρ) was measured from room temperature to 500 K, every 5 degrees, using a 4-point van der Pauw configuration. In order to minimize the effect of delays between the sensed temperature and the actual sample temperature, there was a waiting time of 5 minutes once each preset temperature was reached during the heating and cooling branches. The sample was kept in a low vacuum (∼1 to 10 mTorr) throughout the temperature cycles. The result is presented in the inset of Fig. 3 for one full cycle. As shown, the data values are nearly the same at each temperature in both, the heating and cooling branches of the cycle, so no distinguishable hysteresis was observed. Lack of observed thermal hysteresis is consistent with most previous results for V_3O_5. As mentioned before, it has been found to be either absent or small (i.e., 0.5° or less), even in bulk crystals. This might seem surprising because of the well known case of VO_2 (and, to a lesser degree, V_2O_3), which exhibits a readily measurable hysteresis in bulk crystals, and usually larger (often much larger) widths for thin film samples. The origin of this broadening in VO_2 films is still an active research topic even though it has been studied intensely for many years.[30] In the case of V_3O_5, the lack of readily measurable hysteresis or, more likely, its very small width may be related to the small structural change occurring during the transition, which suggests that the energy barrier between

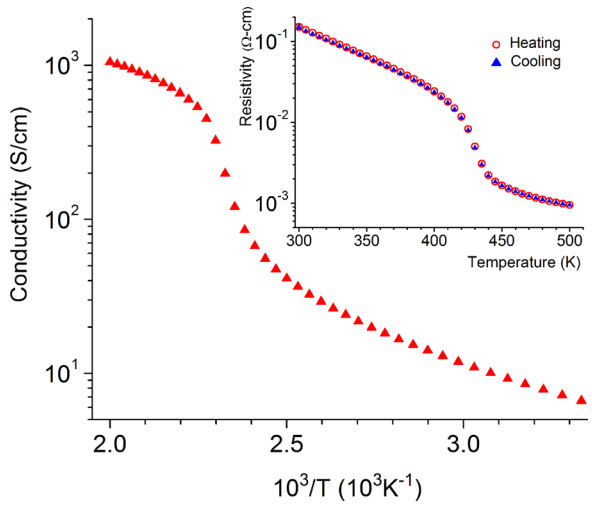

FIG. 3. Inset: resistivity (log scale) as a function of temperature for V_3O_5/glass thin film sample, showing the full heating-cooling cycle. Note the lack of observable hysteresis. Main graph: Arrhenius plot for the same data (only heating branch shown).

the two phases is also small. This particular issue will require further study, particularly since some of the likely technological applications of V_3O_5 in thin film form can benefit from a lack of hysteresis.

Over the 200° temperature range measured, the resistivity changed by more than two orders of magnitude, but the transition can be identified as occurring through a 100° region extending from ~395 to ~465 K. Through this region, the measured resistivity changes by a factor of 20, which is consistent with known characteristics of single crystals, except for the much broader temperature span of the transition in the present case. The steepest change was determined to be by 430 K, for both the heating and cooling branches of the cycle, by calculating the derivative of *log* (ρ) with respect to temperature (see graphs in Fig. S2 in the supplementary material). This value is the same or nearly the same as that found in the literature for bulk V_3O_5 crystals in most cases reported. It is noted also that in all previously reported cases of resistivity measurements for V_3O_5 thin films, all of them produced after annealing treatments in specially prepared atmospheres, the transition temperature has been recorded at lower,[14] or much lower values.[18,19] An Arrhenius plot for the measured conductivity is presented in the main graph in Fig. 3. Because of the lack of observable hysteresis only the heating branch of the cycle is shown here. For temperatures above ~470 K the plot is linear, and an activation energy of 0.16 eV was calculated, which is higher than the 0.13 eV value reported for single crystals.[12] For the lower temperature range (about $T < 340$ K) the Arrhenius plot is also linear, and a slightly lower activation energy of 0.15 eV was calculated.

Resistivity of the sample throughout the full temperature range tested was lower than the reported values for single crystals, but particularly so for the low-temperature phase. At 500 K, for example, $\rho \approx 10^{-3}$ Ω cm, which is just half the value reported for crystals.[31] At room temperature, on the other hand, $\rho = 0.15$ Ω cm, which is two to three orders of magnitude lower than values reported for crystals. It could be thought that the low resistivity may be caused by the V_2O_3 inclusions revealed in the XRD scans. Crystalline V_2O_3 exhibits metallic conduction and a fairly constant $\rho \sim 7 \times 10^{-4}$ Ω cm value for the full temperature range of interest here,[32] up to more than three orders of magnitude lower than all reported results for V_3O_5 crystals at temperatures below the transition. However, application of a simple effective medium approximation model for the measured sample resistivity, using the quoted resistivity value for V_2O_3 and resistivity values for crystalline V_3O_5 in the range of published data leads to V_2O_3 fractions which are unreasonably high (well over 50% by volume) in view of the XRD results for our films, and also inconsistent as the temperature is varied, even if temperature regions considered are only those away from the transition region. We conclude that the volume fraction of V_2O_3 present in the samples, although sufficient to be detectable in the XRD scans for the thicker films, is likely too small to have a significant effect on the measured resistivity and that the low values obtained have a different origin.

As mentioned before, the presence of at least some V_2O_3 suggests that the V_3O_5 in the films is very likely oxygen-deficient and the slightly contracted unit cell, as determined from the XRD results, indicates that oxygen vacancies are the way in which the material accommodates for this deficiency. With respect to the perfect lattice, these vacancies imply positive charges at the defect site, which are compensated by the release of electrons. Using the Kröger–Vink notation, this can be formally described by the reaction $O_O \rightarrow {}^1/_2O_2 + Va_O^{2\bullet} + 2e'$ (where, in order to avoid confusion with the chemical symbol for vanadium, Va stands for "vacancy").[33] Thus, if the band model picture is applied, the oxygen vacancies can be thought to generate shallow states which contribute conduction electrons. In any case, availability of these electrons can explain the high conductivities measured for the films at temperatures below T_c, in comparison to reported single-crystal values. A simple "hot probe" test of the samples, in which the conductivity type is determined by the sign of the Seebeck voltage caused by a thermal gradient established by a heated contact to the sample,[34] evidenced that the majority carriers are negative, as expected from the previous analysis.

The conductance of some vanadium oxides and titanium oxides, which form the Magnéli series, was studied a few decades ago in crystalline samples.[35,36] In these and similar materials, conductivity is low and cannot be readily explained by the band theory. The low carrier mobility in these crystals is attributed to conduction electrons having to overcome potential energy barriers between cation sites. Electrons can either "hop" over the barriers or tunnel through them. Both of these processes are thermally activated, but lead to different temperature dependencies.[37,38] The theory was further developed by Bryksin within the framework of the small-polaron theory, which allows treatment in terms of these quasiparticles instead of the many-body problem arising from interaction between the slow moving electrons and the crystal lattice.[39,40] This theory was recently applied to semiconducting (i.e., below T_c) V_3O_5 single crystals by Andreev and Klimov.[16] However, in the present case, significant concentrations of oxygen vacancies in the thin film samples can provide populations of conduction electrons which are not effectively localized. An additional complication is introduced by the fact that the films are polycrystalline, so that conductivity will be affected as well by extended defects associated with grain boundaries, which can trap carriers and reduce their mobility. Hence no modeling of sample conductivity in terms of theoretical principles was attempted here. In general, however, we expect that deviation from stoichiometry in V_3O_5 thin film samples will have a substantial effect on the conductivity properties for temperatures below T_c and a much smaller effect for temperatures above T_c. As the sample temperature is raised and approaches T_c, conductivity substantially increases, just as in the case of a single-crystal V_3O_5. This can be pictured in terms of overlap of valence and conduction bands or electron delocalization associated with the structural change. As this effect becomes dominant it can explain why the measured conductivities for the samples then become much closer to reported single-crystal values.

If the relatively low resistivity of the V_3O_5 films is indeed caused by oxygen vacancies, as proposed above, it may be expected that heating a sample in an oxidizing atmosphere could decrease the vacancy concentration and thus

increase its resistivity. In order to explore this possibility, the resistivity of a thin (90 nm thick) sample, deposited under nominally the same conditions as described before, was measured continuously while the sample was kept in air at 500 K. This relatively low temperature was chosen because it was known, from previous temperature cycling experiments, that the V_3O_5 film should be able to withstand this temperature in air without transforming into higher oxides. The measured resistivity at 500 K slowly increased, reaching a 12.5% higher value after 6.5 h. The same sample was then continuously subjected to 200 heating-cooling cycles between 300 and 500 K, a process which took a total of nearly 500 h. The results (detailed in the supplementary material, see Fig. S3) showed that resistivity throughout the full temperature range continued to increase, much more slowly so towards the last cycles. The transition temperature, determined as before by calculating the derivative of *log* (ρ) with respect to temperature, did not vary significantly, remaining between 426 and 247 K from the first to the 200th cycle. A XRD scan of the same sample after this treatment did not reveal any peaks which were not attributable to V_3O_5, as before treatment. The observed resistivity increase is larger in relative (i.e., percent) terms for the high-temperature phase (see Fig. S4 in supplementary material). However, it is misleading to focus on the relative change, since initial resistivity values themselves are much lower for the high-temperature phase. In absolute terms the resistivity increases obtained are much higher for the low-temperature phase (see Fig. S5 in supplementary material). In fact the resistivity increase for the 200th cycle, compared with the first, is the largest at 300 K, is gradually lower for each higher temperature, and becomes very low (although still positive) for temperatures higher than the transition temperature. It is noted that, even if the high-temperature resistivity values did not increase very much, these were already not too far from the range of values quoted in the literature for high-V_3O_5 in bulk crystals. On the other hand, even if the low-temperature resistivity values increased significantly after the heating treatment, they are still two to three orders of magnitude lower than reported for V_3O_5 crystals. These results are in general agreement with the idea that the high conductivity of the V_3O_5 film samples in comparison with that of bulk crystals is related to a high concentration of oxygen vacancies in the films. The effect on conductivity of free electrons associated with oxygen vacancies can be expected to be less noticeable for high-V_3O_5 since the contribution of delocalized electrons becomes dominant. In contrast, for low-V_3O_5 localization of *d*-electrons, which is responsible for the low conductivity of nearly stoichiometric bulk crystals, is overwhelmed by the additional conduction electrons contributed by the oxygen vacancies. Detailed understanding of conduction through the phase transition in V_3O_5 films will require more experimental and theoretical work in the future.

OBSERVATION OF ULTRAFAST NONLINEAR OPTICAL (NLO) RESPONSE

In order to explore ultrafast nonlinear optical (NLO) response by the V_3O_5 films, light scattering was measured with a pump-probe technique using 130 fs pulses. A 90 nm thick V_3O_5 sample deposited on SiO_2 glass was used for this purpose. The setup and technique has been well described elsewhere.[41,42] Wavelengths of the pump and probe pulses were, respectively, 800 and 400 nm. The average pump beam energy fluence was 20 mJ/cm^2. Both pump and probe beams were normally incident on the sample surface, with a spot size of 600 μm and 70 μm, respectively. Scattered light was collected over the full front hemisphere by an elliptical mirror and focused on a silicon photodiode. The time delay between pump and probe pulses was controlled by an electromechanical optical delay line. Figure 4 shows the differential signal $\Delta I_S/I_0$ for total integrated scatter relative to the incident light I_0, as a function of time delay for the probe pulse. A prompt reduction was observed in the transient relative scattered light signal, reaching –10% in ~800 fs or less, as seen in the figure inset. This type of response, which is caused by changes in the material's optical constants, is similar to that observed before for VO_2, except in that case the relative change $\Delta I_S/I_0$ is higher (10% to 30%).[43] The strong NLO response observed in the V_3O_5 thin films is very likely related to a photoinduced insulator-to-metal phase transition. However, further study of ultrafast electronic and structural dynamics will be required to elucidate the nature of the observed transient nonlinearity.

In conclusion, deposition of V_3O_5 thin films on SiO_2 glass was achieved directly by DC magnetron sputtering, without any subsequent annealing. From evidence of XRD analysis, the films are oxygen-deficient and this deficiency is accommodated by oxygen vacancies. The film resistivity was measured from 300 to 500 K. The materials' phase transition near ~430 K was clearly observed, with a resistivity change by a factor of 20, and no hysteresis detected in heating-cooling cycles. The high conductivity measured for the films in comparison with published values for V_3O_5 single crystals was attributed to the oxygen vacancies, which can release conduction electrons. This hypothesis was supported by the gradual resistivity increase observed for a sample through 200 thermal cycles, between 300 and 500 K, in air. Further work, including post-deposition

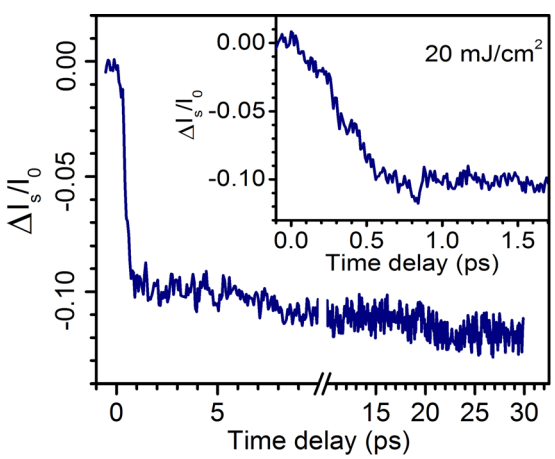

FIG. 4. Main graph: change in total integrated scattered light ΔI_S from a V_3O_5 film, normalized by incident light I_0, as a function of time delay between the pump and probe pulses. The pump beam fluence was 20 mJ/cm^2. Note the break and change of scale in the time scale. Inset: detail for delay times lower than 1.7 ps.

annealing, should lead to production of V_3O_5 or $V_3O_{5-\delta}$ films on glass with reproducible and well-controlled composition within the limits of the material's stoichiometric bounds and, therefore, convenient conductivity values, particularly near room temperature. The fact that the growth technique employed is entirely compatible with standard microelectronic fabrication procedures can enhance interest on this material for applications in CMOS and other devices. Ultrafast NLO response was observed for the films using a pump-probe scattering technique. The observed response, within 800 fs, is sufficiently fast and strong that additional interest in this material, both for fundamental study and technological applications should be stimulated by this report.

SUPPLEMENTARY MATERIAL

See supplementary material for XRD and resistivity vs. temperature measurements.

ACKNOWLEDGMENTS

The authors are pleased to acknowledge support for this work by the U.S. Army Research Office under Award No. W911NF-15-1-0448, and by the UPRM College of Arts and Sciences.

[1]*Landolt-Börnstein: Numerical Data and Functional Relationships in Science and Technology - New Series - Group III Condensed Matter*, edited by H. P. J. Wijn (Springer-Verlag, 1992), Vol. 27G, p. 6.
[2]S. Kachi, K. Kosuge, and H. Okinaka, J. Solid State Chem. **6**, 258 (1973).
[3]Z. Yang, C. Ko, and S. Ramanathan, Annu. Rev. Mater. Res. **41**, 337 (2011).
[4]A. L. Pergament, G. B. Stefanovich, and A. A. Velichko, J. Sel. Top. Nano Electron. Comput. **1**, 24 (2013).
[5]A. Vassighi and M. Sachdev, *Thermal and Power Management of Integrated Circuits* (Springer, NY, 2006).
[6]S. Åsbrink, S. Friberg, A. Magnéli, and G. Andersson, Acta Chem. Scand. **13**, 603 (1959).
[7]S. Åsbrink and S. H. Hong, Nature **279**, 624 (1979).
[8]S. Åsbrink, Acta Cryst., B **36**, 1332 (1980).
[9]N. I. Bogdanova and C. A. Aria, J. Gen. Chem. USSR **30**, 3 (1960).
[10]E. I. Terukov and F. A. Chudnovskii, Fiz. Tekh. Poluprovodn. **8**, 1226 (1974).
[11]E. I. Terukov, F. A. Chudnovskii, W. Reichelt, H. Oppermann, W. Brückner, H. P. Brückner, and W. Moldenhauer, Phys. Status Solidi A **37**, 541 (1976).
[12]E. I. Terukov, D. I. Khomskii, and F. A. Chudnovskii, J. Exp. Theor. Phys. **46**, 1160 (1977).
[13]J. M. Honig, J. Solid State Chem. **45**, 1 (1982).
[14]N. N. Khoi, T. R. Simon, and H. K. Eastwood, Mater. Res. Bull. **11**, 873 (1976).
[15]H. Jhans and J. M. Honig, J. Solid State Chem. **38**, 112 (1981).
[16]V. N. Andreev and V. A. Klimov, Phys. Solid State **53**, 2424 (2011).
[17]B. Fisher, L. Patlagan, K. B. Chashka, C. Makarov, and G. M. Reisner, Appl. Phys. Lett. **109**, 103501 (2016).
[18]L. A. Beresneva, S. F. Devyatova, and L. L. Vasilyeva, Thin Solid Films **75**, 47 (1981).
[19]M. A. Abdullaev, I. K. Kamilov, and E. I. Terukov, Inorg. Mater. **37**, 271 (2001).
[20]J. Musil, P. Baroch, J. Vlček, K. H. Nam, and J. G. Han, Thin Solid Films **475**, 208 (2005).
[21]Powder Diffraction File 72-0977, International Centre for Diffraction Data, PA, USA.
[22]Powder Diffraction File 85-1411, International Centre for Diffraction Data, PA, USA.
[23]Y. B. Kang, J. Eur. Ceram. Soc. **32**, 3187 (2012).
[24]Y. Cui, B. Liu, L. Chen, H. Luo, and Y. Gao, AIP Adv. **6**, 105301 (2016).
[25]I. Petrov, I. Ivanov, V. Orlinov, and J.-E. Sundgren, J. Vac. Sci. Technol. A **11**, 2733 (1993).
[26]B. A. Movchan and A. V. Demchishin, Phys. Met. Metallogr. **28**, 653 (1969).
[27]J. A. Thornton, Ann. Rev. Mater. Sci. **7**, 239 (1977).
[28]E. Mirica, G. Kowach, and H. Du, Cryst. Growth Des. **4**, 157 (2004).
[29]H. A. Wriedt, "The O-V (Oxygen-Vanadium) system," in *Phase Diagrams of Binary Vanadium Alloys*, edited by J. F. Smith (ASM International, 1989).
[30]J.-G. Ramírez, A. Sharoni, Y. Dubi, M. E. Gómez, and I. K. Schuller, Phys. Rev. B **79**, 235110 (2009).
[31]F. A. Chudnovskii, J. Phys. C: Solid State Phys. **11**, L99 (1978).
[32]J. Feinleib and W. Paul, Phys. Rev. B **155**, 841 (1967).
[33]*Nomenclature of Inorganic Chemistry, IUPAC Recommendations 2005*, edited by N. G. Connelly, R. M. Hartshorn, T. Damhus, and A. T. Hutton (International Union of Pure and Applied Chemistry/RSC Publishing, 2005).
[34]D. K. Schroder, *Semiconductor Material and Device Characterization* (John Wiley & Sons, 1990), p. 30.
[35]A. D. Inglis, Y. L. Page, P. Strobel, and C. M. Hurd, J. Phys. C: Solid State Phys. **16**, 317 (1983).
[36]A. D. Inglis, C. M. Hurd, and P. Strobel, J. Phys. C: Solid State Phys. **17**, 6801 (1984).
[37]R. H. Tredgold, Proc. Phys. Soc. **80**, 807 (1962).
[38]C. M. Hurd, J. Phys. C: Solid State Phys. **18**, 6487 (1985).
[39]V. V. Bryksin, J. Exp. Theor. Phys. **73**, 861 (1991).
[40]V. V. Bryksin, J. Exp. Theor. Phys. **74**, 97 (1992).
[41]S. Lysenko, F. Fernández, A. Rúa, and H. Liu, J. Appl. Phys. **114**, 153514 (2013).
[42]S. Lysenko, F. Fernández, A. Rúa, N. Sepúlveda, and J. Aparicio, Appl. Opt. **54**, 2141 (2015).
[43]S. Lysenko, A. Rúa, F. Fernández, and H. Liu, J. Appl. Phys. **105**, 043502 (2009).